Analysis of optical response of long period fiber gratings to nm-thick thin-film coatings

Zhiyong Wang

Department of Electrical Engineering, Virginia Tech, Blacksburg, VA 24061, USA
zhwang@vt.edu

J. R. Heflin

Department of Physics, Virginia Tech, Blacksburg, VA 24061, USA
rheflin@vt.edu

Rogers H. Stolen

Department of Electrical Engineering, Virginia Tech, Blacksburg, VA 24061, USA

Siddharth Ramachandran

OFS Laboratories, 25 Schoolhouse Road, Somerset, NJ 08873, USA
sidr@ieee.org

Abstract: We have theoretically and experimentally demonstrated that the resonant wavelength of long period fiber gratings (LPG) can be shifted by a large magnitude by coating with only a nm-thick thin-film that has a refractive index higher than that of the glass cladding. The resonant wavelength shift can result from either the variation of the thickness of the film and/or the variation of its refractive index. These results demonstrate the sensitivity of LPG-based sensors can be enhanced by using a film of nm-thickness and refractive index greater than silica. This coating schematic offers an efficient platform for achieving high-performance index-modulating fiber devices and high-performance index/thickness-sensing LPG-based fiber sensors for detecting optical property variations of the thin-film coating.

©2005 Optical Society of America

OCIS codes: (060.2370) Fiber optics sensors; (060.2340) Fiber optics components; (350.2770) Gratings; (310.0310) Thin films

---

References and links

1. M. Vengsarkar, P. J. Lemaire, G. Jacobovitz-Veselka, V. Bhatia, and J. B. Judkins, "Long-period fiber gratings as gain-flattening and laser stabilizing devices," Proc. IOOC'95, PD1–2 (1995).
2. S. Ramachandran, S. Ghalmi, Z. Wang, and M. Yan, "Band-Selection Filters using Concatenated Long-Period Gratings in Few-mode Fibers," Opt. Lett. **27**, 1678-1680 (2002).
3. S. Ramachandran, Z. Wang, M. Yan, "Bandwidth control of long-period grating-based mode converters in few-mode fibers," Opt. Lett. **27**, 698-700 (2002).
4. H. J. Patrick, A. D. Kersey, and F. Bucholtz, "Analysis of the response of long period fiber gratings to the external index of refraction," J. Lightwave Technol. **16**, 1606-1612 (1998).
5. B. Acharya, T. Krupenkin, S. Ramachandran, Z. Wang, C. Huang, and J. Rogers, "Tunable optical fiber devices based on broadband long-period gratings and pumped microfluidics," Appl. Phys. Lett. **83**, 4912-4914 (2003).
6. Z. Wang and S. Ramachandran, "Ultra-Sensitive Long Period Fiber Gratings for Broadband Modulators and Sensors," Opt. Lett. **28**, 2458-2460 (2003).
7. N. Rees, S. James, R. Tatam, G. Ashwell, "Optical fiber long-period gratings with Langmuir-Blodgett thin-film overlays," Opt. Lett. **27**, 686-688 (2002).
8. Z. Wang, J. R. Heflin, R. H. Stolen, N. Goel and S. Ramachandran, "Sensitive optical response of long period fiber gratings to nm-thick ionic self-assembled multilayers," Proc. CLEO'04, CWD2, (2004).
9. Z. Wang, J. R. Heflin, R. H. Stolen, and S. Ramachandran, "Highly sensitive optical response of optical fiber long period gratings to nm-thick ionic self-assembled multilayers," Appl. Phys. Lett. (to be published).

10. Decher, "Fuzzy Nanoassemblies: Toward Layered Polymeric Multicomposites,",Science **277**, 1232-1235 (1997).
11. J.R. Heflin, C. Figura, D. Marciu, Y. Liu, R. Claus, "Thickness dependence of second-harmonic generation in thin films fabricated from ionically self-assembled monolayers," Appl. Phys. Lett. **74**, 495-497 (1999).
12. I. Del Villar, I. R. Matías, F. J. Arregui, and P. Lalanne, "Optimization of sensitivity in Long Period Fiber Gratings with overlay deposition," Opt. Express **13**, 56-69 (2005)
13. D. Marcuse, *Theory of Dielectric Optical Waveguides* (New York: Academic, 1991).
14. Turan Erdogan, "Fiber grating spectra," J. Lightwave Technol. **15**, 1277-1294 (1997).

1. Introduction

Long-period fiber gratings (LPG) couple light between copropagating modes of an optical fiber. They have been broadly used as spectral shapers [1,2] and mode converters [3] in optical fiber communication systems because of their characteristics such as compactness, low insertion loss and low back reflection. In addition, single-mode fiber (SMF)-based LPGs have been extensively investigated for use as chemical [4] or biological sensors and other index-modulating fiber devices [5,6] due to their high resolution and sensitivity to the refractive index of the material surrounding the fiber.

Recently, Rees [7] and we [8,9] have reported the resonant wavelength shift of an LPG in response to a thin-film coating of sub-wavelength thickness by utilizing the Langmuir-Blodgett (LB) technique and ionic self-assembled multilayers (ISAM) technique, respectively. Because LB thin-films have relatively poor mechanical and thermal stability, the ISAM technique is more suitable for practical devices due to its enhanced reliability, tunability and film quality. The ISAM technique [10,11] provides a highly controllable means to build precise, nm-thick films on any charged surface such as glass, silicon, metal, etc. Furthermore, a diverse array of materials (e.g. nanoparticles, proteins, virus particles etc.) can be incorporated into ISAM films. Hence, ISAMs adsorbed on LPGs provide a potentially robust platform for building efficient sensors which could sense variations induced by optical property changes of nm-thick surrounding media. Because the sensing element of a practical LPG-based chemical/biological sensor would often be a nm-thick thin-film coated on the surface of the LPG where the thin-film is synthesized by incorporating sensing chemical/biological molecules into it, it is important to investigate the sensitivity of the LPG upon variations of the thickness and/or the index of the sensing thin-film for this type of thin-film coated LPG. More recently, Del Villar et al. [12] reported that the sensitivity of LPG sensors could be improved by selecting an optimum film thickness. Their analysis showed that cladding modes transition from being guided in the glass cladding to residing predominantly in the film coating, and that maximum sensitivity is obtained for a thickness where this transition occurs.

There are other parameters that also control the sensitivity of thin-film-coated LPGs, such as the cladding mode order and index of the film. This report is a detailed study of LPG sensitivities when they are coated with nm-thick films of refractive index higher than silica. Specifically, we consider the influence of cladding mode order, and show that resonant wavelength shifts due to similar film-coating thickness and refractive index values, can be vastly different, depending on the cladding mode to which the LPG induces coupling. We verify the qualitative conclusions from the theoretical analysis by comparing them with experimental results of the response of an ISAM-coated LPG that couples to a very high order cladding mode ($LP_{0,12}$). The dramatic range of sensitivities accessible by proper choice of cladding mode order makes this technological platform very attractive for a variety of index modulating and sensing applications.

2. Theoretical analysis of nm-thick thin-film coated LPG

An LPG is an optical fiber with ultraviolet (UV)-induced modulations of the refractive index of the fiber core, with a typical period of larger than 100 μm and length of a few cm. In the case of our interest, the fiber cladding of an SMF-based LPG is coated by a nm-thick thin-film whose refractive index is higher than that of the cladding glass. The step-index approximation

was adopted in our LPG structure modeling. The illustrative schematic of the thin-film coated LPG structure is shown in Fig. 1(a). Figure 1(b) depicts the refractive index profile of this LPG structure correspondingly, n_1 is the index of fiber core, n_2 is the index of fiber cladding, n_3 is the index of nm-thick thin-film, n_{air} is the index of air (n_{air}=1) and $n_3 > n_1 > n_2 > n_{air}$. To simulate the material dispersion of the germanium-doped glass fiber, we calculated n_1 and n_2 based on Sellmeier's equation [13].
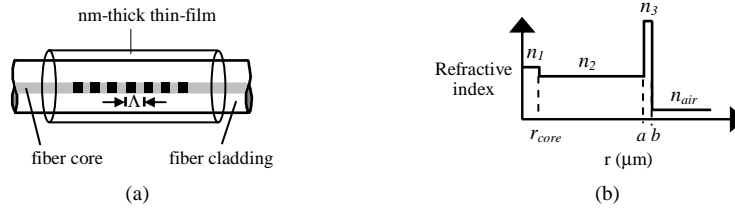

Fig. 1. (a) Illustrative schematic of LPG with an nm-thick thin-film coating (b) Index profile of the thin-film coated LPG, n_1 is index of fiber core, n_2 is index of fiber cladding, n_3 is index of the thin-film, n_{air} is index of air, and $n_3 > n_1 > n_2 > n_{air}$. Thickness d of the film is denoted $d = b-a$.

The LPG couples light from the fundamental mode into its cladding modes described by the resonant condition equation: $\lambda_m = (n_{core} - n_{0m})\, \Lambda$, where λ_m is the resonant wavelength for the coupled cladding mode $LP_{0,m}$, Λ is the grating period, n_{core} and n_{0m} are the effective index of the fundamental mode $LP_{0,1}$ and the cladding mode $LP_{0,m}$, respectively. The scalar mode theory was employed in our analysis for solving n_{core} and n_{0m} [13], and we followed Erdogan's analysis [14] to simulate the transmission spectra of LPGs.

Based on the resonant condition equation, we can plot a phase-matching-curve (PMC) which depicts Λ as a function of λ_m. In our experiments, the LPGs we used couple the fundamental mode to the cladding mode $LP_{0,12}$ at λ_{12}=1420 nm. In addition, it possesses a Turn Around Point (TAP) in its PMC [3]. To improve our modeling accuracy, we examined the TAP of the grating. By adjusting the radius a of the fiber cladding, we found that the matching between the measured TAP (1500nm) and the calculated TAP occurs at a =59.2 μm instead of standard 62.5 μm. Since the operating wavelength of the grating is relatively far away (~ 80 nm) from the TAP in contrast to the FWHM bandwidth of the grating (~ 12 nm), the grating was operated as a conventional narrow-band LPG. Additionally, we also examined the single-mode operating condition by calculating the cutoff wavelength λ_{cut} of the fiber mode $LP_{1,1}$. Through adjusting the radius r_{core} of the fiber core and the core-cladding index difference used in the step-index profile, we intended to match the calculated λ_{cut} with the measured λ_{cut} (1275 nm). The matching occurred when r_{core} =3.2 μm and the core-cladding index difference was 0.0078 at λ=1300 nm.

To investigate effects of the thickness d ($d = b-a$ as shown in Fig. 1(b)) and the refractive index n_3 of the nm-thick thin-film on LPGs, we first simulated PMC and spectral variations of the grating by altering d and/or n_3. For n_3, we ignored its material dispersion for simplicity and selected four typical values (n_3=1.5, 1.6, 1.7, 1.8), which are within the refractive index range of polymers used for fabricating ISAM films. For d, we chose d=0, 20, 40, 60, 80 and 100 nm which are typical values of thickness of the ISAM film. We selected two typical cladding modes $LP_{0,4}$ and $LP_{0,12}$ to illustrate the low-order and the high-order cladding modes' behaviors.

Figure 2 shows simulated PMC shifts as functions of d and/or n_3 of the thin-film, respectively. Figure 3 shows the corresponding simulated LPG spectral shifts for conditions depicted in Fig. 2. To be comparable, the criterion for choosing periods for $LP_{0,4}$ and $LP_{0,12}$ was to set resonant wavelengths of $LP_{0,4}$ and $LP_{0,12}$ to be $\lambda_4 = \lambda_{12}$=1420nm which is the resonant wavelength of our experimental LPG.
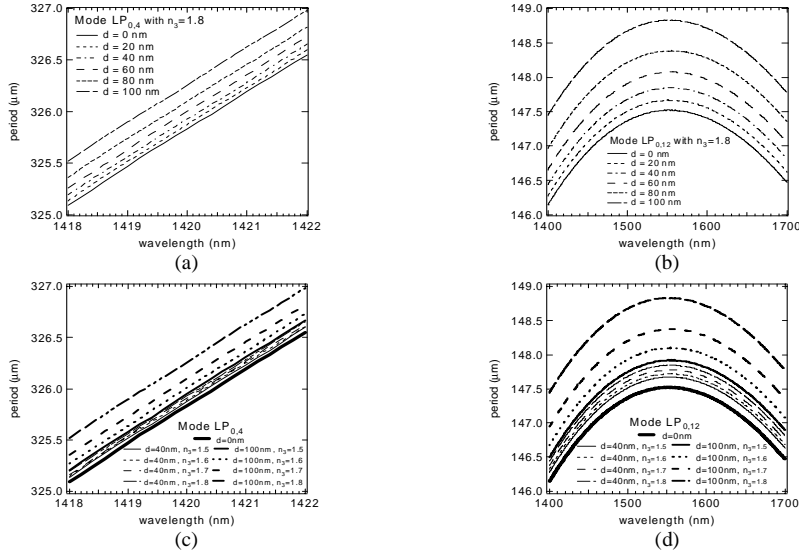
Fig. 2. Phase Matching Curves (PMC) shifts as functions of index n_3 and thickness d of nm-thick thin-film (a) PMC of $LP_{0,4}$ mode shifts with d (0, 20, 40, 60, 80, 100nm) at n_3=1.8, (b) PMC of $LP_{0,12}$ mode shifts with d (0, 20, 40, 60, 80, 100nm) at n_3=1.8, (c) PMC of $LP_{0,4}$ mode shifts with n_3 (1.5, 1.6, 1.7, 1.8) at d=40nm and d=100nm, (d) PMC of $LP_{0,12}$ mode shifts with n_3 (1.5, 1.6, 1.7, 1.8) at d=40nm and d=100nm.
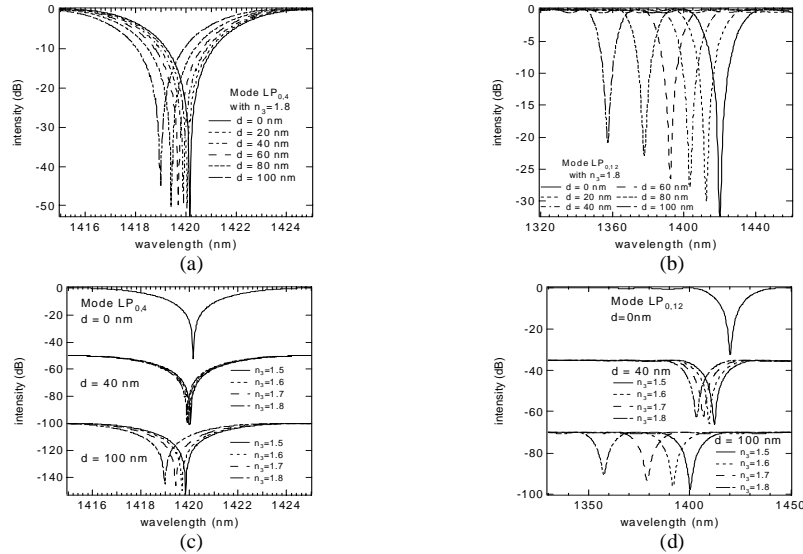

Fig. 3. LPG spectra shifts as functions of index n_3 and thickness d of nm-thick thin-film (a) spectra of $LP_{0,4}$ mode shifts with d (0, 20, 40, 60, 80, 100nm) at n_3=1.8, (b) spectra of $LP_{0,12}$ mode shifts with d (0, 20, 40, 60, 80, 100nm) at n_3=1.8, (c) spectra of $LP_{0,4}$ mode shifts with n_3 (1.5, 1.6, 1.7, 1.8) at d=40nm and d=100nm, (d) spectra of $LP_{0,12}$ mode shifts with n_3 (1.5, 1.6, 1.7, 1.8) at d=40nm and d=100nm.

According to simulations as shown in Fig. 3, we note that: (i) when n_3 is fixed, the spectra of $LP_{0,4}$ and $LP_{0,12}$ shift towards shorter wavelengths as d increases. The spectral shift gradually increases as d is increased from 0 nm to 100 nm (e.g. for n_3=1.8 as shown in Fig. 3(b), a resonant-wavelength shift of ~ 9 nm is obtained for a change in d from 20 nm to 40 nm, but the corresponding resonant-wavelength-shift is ~ 20 nm when d is increased by the same amount from 80 nm to 100 nm). This means that the sensitivity to d increases with d; (ii) For fixed d, the $LP_{0,4}$ and $LP_{0,12}$ resonances shift to longer wavelengths as n_3 increases, and the

rate of change increases with the magnitude of n_3 (e.g. for $d = 100$ nm as shown in Fig. 3(d), a resonant-wavelength shift of ~ 9 nm is obtained when n_3 is increased from 1.5 to 1.6, but a wavelength shift of ~ 20 nm is obtained when n_3 is increased from 1.7 to 1.8) which means the sensitivity to n_3 increases as n_3 increases;. (iii) When d is fixed, the spectra shift leftwards as n_3 increases. The magnitude of the spectral shift upon each 0.1 increment of n_3 is obviously larger at larger d (e.g. as shown in Fig. 3(d), a wavelength shift of ~ 3 nm is obtained at $d = 40$ nm when n_3 is increased from 1.7 to 1.8, but a wavelength shift of ~ 20 nm is obtained at $d = 100$ nm under the same condition), which means the sensitivity to n_3 increases as d increases; (iv) For either fixed d or n_3, the spectrum of $LP_{0,12}$ shifts much more than that of $LP_{0,4}$, which means the sensitivity of $LP_{0,12}$ to d and n_3 is much higher than that of $LP_{0,4}$. The enhanced sensitivity of higher order cladding modes is due to two factors: the PMC of the higher order mode has smaller gradient (operates closer to the TAP), which implies that small changes in any parameter lead to large resonant-wavelength shifts. Secondly, a higher order mode interrogates material further from the core of the fiber, and hence changes in film thicknesses and refractive indices far from the core have a larger effect. Furthermore, although the thickness of the thin-film is at only the nanometer level, the resonant wavelength of the LPG can be shifted by more than 60 nm for $LP_{0,12}$ as shown in Fig. 3(b).

3. Experimental results

We now compare the theoretical predictions from the last section, with experiments on ISAM coated LPGs that induce coupling a higher order cladding mode, namely the $LP_{0,12}$ mode. In our experiments, the LPGs were UV-induced on TrueWave RS™ SMFs with a grating period of 116 μm and a length of 5 cm. This yielded gratings that couple the fundamental mode to the $LP_{0,12}$ cladding mode at $\lambda_{12}=1420$ nm. d and n_3 of ISAM films were measured by ellipsometry [8,9]. Different pH combinations of polycation (PAH) and polyanion (PCBS) result in different d and n_3 of the PAH/PCBS-based ISAM films [8,9]. Ranges of d and n_3 are from 0 nm to 60 nm and from 1.67 to 1.72, respectively.

Figure 4(a) shows the comparison between the experimental and the simulated LPG spectrum without the ISAM film coating. They are in good agreement. Figure 4(b) shows typical experimental LPG spectra as a function of different PAH/PCBS bilayers (i.e. different thicknesses) of ISAM films for PAH solution at pH=7.5 and PCBS solution at pH=8.0. Here one PAH/PCBS bilayer is ~1.3 nm in thickness.

Finally, Fig. 5 shows the experimental results of the resonant wavelength shifts $\Delta\lambda_{res}$ of the ISAM coated LPG as a function of the thickness d of ISAM films (different pH combinations of PAH and PCBS [(7.5,6), (7.5,8), (9,6), (9,8)] result in different values for n_3 [1.7107, 1.6912, 1.6887, 1.6715], respectively). In Fig. 5 each $\Delta\lambda_{res}$-versus-d curve is for a fixed n_3 obtained from a fixed pH-combination of PAH and PCBS. We note that experimental results exhibit: (i) for fixed n_3, $\Delta\lambda_{res}$ gradually increases with increased d (e.g. for $n_3=1.7107$ [curve (7.5,6)]) - a wavelength shift of ~ 12 nm is obtained when d is increased from the first data point to the second data point by ~ 8 nm, but a wavelength shift of ~ 18 nm is obtained when d is increased from the second data point to the third data point by the same increment. Other curves show the same behavior.; (ii) for fixed d, $\Delta\lambda_{res}$ increases as n_3 increases {e.g. for $d = 25$ nm, a wavelength shift of ~ 7 nm is obtained when n_3 is increased from 1.67 [curve(9,8)] to 1.69 [curve(7.5,8)] by ~ 0.2, but a wavelength shift of a wavelength shift of ~ 20 nm is obtained when n_3 is increased from 1.69 [curve (7.5,8)] to 1.71 [curve (7.5,6)] by ~ 0.2}; (iii) for fixed d, the magnitude of $\Delta\lambda_{res}$ upon fixed increment of n_3 is obviously larger at larger d {e.g. a wavelength shift of ~ 8 nm is obtained at $d = 10$ nm when n_3 is increased from 1.67 [curve(9,8)] to 1.71 [curve (7.5,6)] by ~ 0.4, but a wavelength shift of ~ 20 nm is obtained at $d = 20$ nm under the same condition}. The result of (i) means the sensitivity to the thickness becomes gradually higher with increased thickness, and the results of (ii) and (iii) mean the sensitivity of the cladding mode to the thickness/index of the ambient thin-film increases as the index/thickness of the ambient thin-film increases, respectively. These results qualitatively agree with the preceding theoretical analysis.

In practical LPG-based sensor applications, the thin-film will most often serve as the sensing element by incorporating sensing chemical/biological molecules into it. An LPG serves as an optical transducer for signaling the occurrence of a chemical/biological interaction event of interest. Here we could obtain a guideline for building efficient LPG-based sensors for practical use as follows: first we need to consider the precondition of this type of thin-film coated LPG-based sensors. Reference [7] shows that the coupled guided cladding mode would cut off and turn into a leaky cladding mode when the LPG is coated with an thin-film whose refractive index is higher than that of the cladding glass and thickness is larger than a cutoff thickness d_{cut}. In such case, a substantially weak resonance is obtained [4]. This is because a leaky mode is not guided due to total internal reflection, but exists because of (weak) Fresnel reflections at the glass-thin-film boundary. Therefore, in this case, the thin-film coated LPG is not suited for sensing applications. Hence, the precondition of this type of thin-film coated LPG-based sensor is to guarantee the existence of the coupled guided cladding mode, and we can achieve it by coating the LPG with a thin-film of a thickness smaller than d_{cut}. Then, in order to enhance the sensitivity of the LPG, the thickness of the thin-film should approach d_{cut} as close as possible. In addition, the materials for synthesizing the thin-film should have a high refractive index - i.e. both the ISAM film as well as the sensing molecules should have index greater than silica. Furthermore, this guideline for building efficient sensors is also helpful for building efficient LPG-based modulating devices.
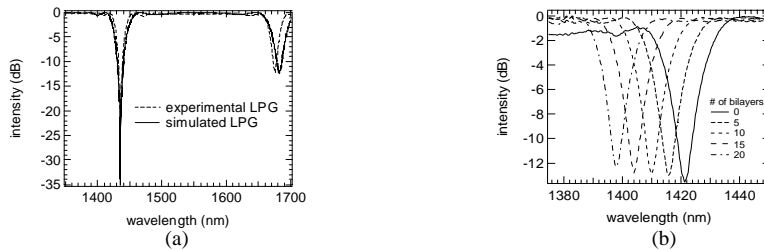

Fig. 4. (a) Comparison between experimental and simulated LPG spectrum without ISAM coating (b) Experimental LPG spectra with 0, 5, 10, 15 and 20 PAH/PCBS bilayers of ISAM films for PAH at pH=7.5 and PCBS at pH= 8.0. One bilayers ≈ 1.3 nm in thickness.
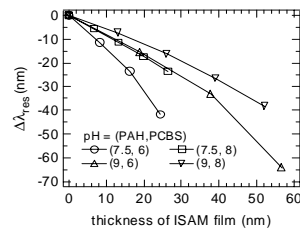

Fig. 5. Experimental results of $\Delta\lambda_{res}$ of ISAM–coated LPG as a function of thickness d of ISAM films (different pH combinations of PAH and PCBS [(7.5,6), (7.5,8), (9,6), (9,8)] offer corresponding index n_3 [1.7107, 1.6912, 1.6887, 1.6715], respectively).

4. Conclusion

In summary, we show that the resonance of the LPG can be tuned by a large magnitude with coatings of only nm-thick thin-films whose indices are higher than that of the glass cladding. The LPG sensitivity critically depends on the modal order to which they couple. The origin of the resonance shift can be either the variation of the thickness of the thin-film and/or the variation of the index of the thin-film. The theoretical analyses as well as experimental data suggest that the sensitivity of LPG-based chemical/biosensors can be improved by appropriate choice of cladding mode order, film thickness, and index. This schematic provides an efficient platform for building index/thickness-sensing LPG sensors for monitoring optical property variations of the sensing thin-film coating as well as index-modulating fiber devices.